International Journal of Applied and Natural Sciences
ISSN: 3005-3471
DOI: 10.61424/ijans
Journal Homepage: www.bluemarkpublishers.com/index.php/IJANS

IJANS
BLUEMARK PUBLISHERS

| RESEARCH ARTICLE

Date Palm Stone Pyrolysis and Gasification in a Bubbling Fluidized Bed Reactor

Abbas Al-Farraji[1] and Haidar Taofeeq[2] ✉
[1]*Chemical Engineering Department, College of Engineering, Al-Nahrain University, Al-Jadriya, Baghdad, Iraq*
[2]*Chemical and Biochemical Engineering, Missouri University of Science and Technology, Rolla, MO 65409, USA*
Corresponding Author: Haidar Taofeeq, **E-mail**: htaofeeq2012@my.fit.edu

| ABSTRACT
The objective of this study is to investigate the potential of agricultural waste feedstock's as a biomass source. A large lab scale thermal-gravimetric fluidized bed reactor (TGFBR) was used to deduce kinetic parameters through measuring the dynamic mass changes of the overall thermal decomposition of biomass under isothermal conditions. The pyrolysis of date palm stones was studied in the TGFBR, and the kinetic expression was determined using a model fitting method. This work reveals that the reaction mechanism of the experimental thermal decomposition of palm stones was three-dimensional diffusion. The activation energy for experiments between 350°C and 600°C was 27.67 kJ/mole. By monitoring the mass variation from pyrolysis tests at different superficial velocities, the TGFBR also allowed deeper insight into suppression of diffusion control during thermal decomposition of biomass. To evaluate the effects of equivalence ratio (ER) and temperature on the product gas, the gasification of date palm stones was investigated at ER (0.15-0.35) and a temperature range of 600-750°C in 50°C increments. The hydrogen and carbon monoxide percentage, and heating value of the product gas, both increase with the increase in gasification temperature. Based on the energy yield (7 MJ/kg), the current results suggested that the optimum conditions were at T=750°C and ER=0.2. The information regarding pyrolysis and gasification is anticipated to be useful for researchers and end users, as well as drawing attention to date palm stones as an agricultural residue, which are valuable for use in alternative energy.

| KEYWORDS
Biomass; Pyrolysis; Gasification; Fluidized bed; Gasifier, Thermal-gravimetric fluidized bed reactor.

| ARTICLE INFORMATION
ACCEPTED: 23 July 2025 **PUBLISHED:** 14 October 2025 **DOI:** 10.61424/ijans.v3.i3.446

1. Introduction
The objective of this study is to investigate the potential of agricultural waste feedstock's as a biomass source. Although this biomass is abundantly available in the country, it remains underutilized in energy recovery applications. Developing countries, whose economies are largely dependent on agriculture and forestry, have shown significant interest in using biomass as an alternative energy source [Al-Farraji, 2017].

Many countries should focus on utilizing all its available resources to foster sustainable growth. Also, these countries should try to not heavily rely only on oil and gas resources to meet its electricity demand. However, there has been a steady increase in carbon emissions associated with fossil fuel usage, with a particularly sharp rise observed in recent years [Ahmed, 2011]. As per the author's statement, CO_2 emissions surpassed 2010 levels in 2011 due to the growing dependence on fossil fuels. The heavy use of oil has led to air pollutant levels that exceed international standards, posing a serious threat to public health [Al-Aasadi, 2015]. Additionally, higher levels of

pollution have resulted from the increasing number of vehicles, manufacturing facilities, major industrial zones, and office buildings. To address this pollution problem, other experts have explored the status and potential of renewable energy and have discovered that solar, wind, and biomass sources could play a significant role in the future and help alleviate power shortages in the sector [Kazem, 2012]. In addition, these countries have substantial untapped alternative energy reserves such as date palm tree. Recent studies reveal that these countries collectively contain 70% (equal to 120 million) of the world's date palms and are responsible for 67% of the total worldwide date production [Al-Farraji, 2017, El-Juhany, 2010]. The estimated total annual production of dates [Erskine, 2004]. When date palm fruits are processed, a considerable amount of date palm stones is produced as waste materials. These unwanted stones can cause severe environmental problems like attracting insects, diseases, and fire hazards. Interestingly, these date stones make up approximately one-third of the weight of the date fruit, making it an untapped resource that can be used as a source of energy. Therefore, it is essential to discover new technologies capable of exploiting this biofuel as energy while minimizing emissions. Moreover, date stones have a higher density (560 kg/m3) and can be used without densification, which can significantly reduce pre-processing costs. [Sait, 2012].

One of the essential thermochemical technologies used for converting biomass into energy is pyrolysis and gasification. The products derived by pyrolysis are mostly influenced by the operating circumstances, such as temperature, heating rate, and residence time. These conditions can be modified to achieve the desired output. Fast pyrolysis, which involves high heating rates, moderate temperatures, and short residence times, produces more liquids and volatiles than char. These liquids can replace fuel oil for electricity generation or heating purposes. [Xianwen, 2000].

The design of a reactor requires the determination of kinetic parameters such as activation energy and rate constant k, in order to optimize the reaction conditions [Jeguirim, 2014]. While benchtop thermogravimetric analysis (TGA) is commonly used for studying biomass reactivity, it has some limitations such as small sample sizes, mass transfer control, and low heating rates that may affect the relevance of results. Other researchers have also noted that the heating rate in a TGA is insufficient to simulate the high heating rates in fluidized bed or circulating bed reactors [Al-Farraji, 2017, Lv, 2004]. Thus, there is a need to develop energy conversion systems that can provide reliable kinetic data for industrial applications by overcoming limitations such as diffusion rate, heating rate, and sample size. A new thermal-gravimetric fluidized bed reactor has been designed to simulate conditions that are representative of industrial-scale operations, taking into account the effects of sample size, high heating rate, and mass transfer. This highlights the importance of developing efficient energy conversion systems that can provide accurate kinetic data for the successful industrial application of biomass [Al-Farraji, 2017].

Besides biomass pyrolysis, biomass gasification is also significant for the global energy infrastructure as it has the potential to produce various types of biofuel gases and intermediate products. The product gas obtained from the gasification process can be utilized for electricity generation in turbines, combustion for heat generation, or in engines. The composition of the product gas produced during gasification depends on the combination of several gas-solid and gas-gas reactions, which can be represented by reactions (R1) - (R10). The typical reactions that occur during biomass gasification in a fluidized bed are as follows:

Pyrolysis biomass→$char + tar + gases\ (H_2 + CO + CO_2 + CH_4 + C_nH_m)$		R_1
Tar→$CO_2 + CO + H_2 + CH_4 + Light\ H/C$		R_2
Water-gas		
$C + H_2O \rightarrow CO + H_2$	+131 kJ/mol	R_3
Boudouard		
$C + CO_2 \rightarrow 2CO$	+172 kJ/mol	R_4
Oxidation reaction		
$C + 0 \cdot 5O_2 \rightarrow CO$	-111 kJ/mol	R_5
$C + O_2 \rightarrow CO_2$	-394 kJ/mol	R_6
Water-gas shift reaction		
$CO + H_2O \leftrightarrow CO_2 + H_2$	-4198 kJ/mol	R_7
Dry reforming		
$CH_4 + CO_2 \leftrightarrow 2CO + 2H_2$	+247 kJ/mol	R_8
Methanation reaction		
$C + 2H_2 \rightarrow CH_4$	-75 kJ/mol	R_9
$C_nH_m(tar) + nCO_2 \rightarrow (^m/_2)H_2 + 2nCO$	Endothermic	R_{10}

At higher equivalence ratios, the amount of oxygen available increases, which results in the occurrence of oxidation reactions for H_2 and CO, represented by reactions R11 and R12, respectively [Abdoulmoumine, 2014]:

$\mathrm{H_2 + 0.5O_2 \rightarrow H_2O}$	R_{11}
$\mathrm{CO + 0.5O_2 \rightarrow CO_2}$	R_{12}

The primary objectives of this study were twofold: firstly, to investigate the kinetics of pyrolysis of palm stones in a TGFBR, and secondly, to evaluate the feasibility of utilizing date palm stones in a gasification process for energy production by examining the effects of operating conditions. The findings from this research will aid in determining the necessary conditions for operating a reactor in a pilot plant and evaluate the feasibility of using Iraqi palm stones in gasification.

1.1 Date Palm Stone

Iraqi date palm was the source of date palm stones which were around 20-25 mm long and 6-8 mm thick. Due to their large size, it was not easy to fluidize them and regulate the feeding rate. To solve this issue, the date palm stones were dried and then crushed with a Retsch model BB20 crushing machine to particle sizes of 2-4 mm, which made them suitable for pyrolysis and gasification testing.

The proximate analysis was determined according to ISO DIS 18134 (14774-3) (moisture content), BS EN ISO 15148:2009: (volatile matter content) and BS EN 14775:2009 (ash content). Fixed carbon (FC) was calculated 'by difference'. Table 1 illustrates the proximate and ultimate analysis of biomass.

Table 1: Proximate and Ultimate analysis of Date palm stones.

Ultimate analysis		**Proximate analysis**	
Palm stone (wt.%, dry basis)		Palm stone (wt.%, wet basis)	
C	48.68	Fixed carbon	6.73
H	6.6	Volatile matter	82.27
N	0.77	Ash	1.45
S	0.075	Moisture	9.55
O	42.3	HHV_f ($MJkg^{-1}$)	20.4
Ash	1.58		

2. Experimental Facility

In this study, the pilot scale thermogravimetric fluidized bed reactor (TGFBR) used was depicted in Figure 1. The TGFBR was developed at Cardiff University's School of Engineering and consists of various parts such as a biomass feeding system, an air delivery system, a fluidized bed reactor composed of plenum and perforated distributor plate, a heating system comprising a split furnace and preheater, downstream gas cleaning, and product gas analysis. A previous study provides a detailed description of the TGFBR [Al-Farraji, 2017, Marsh R., 2017].

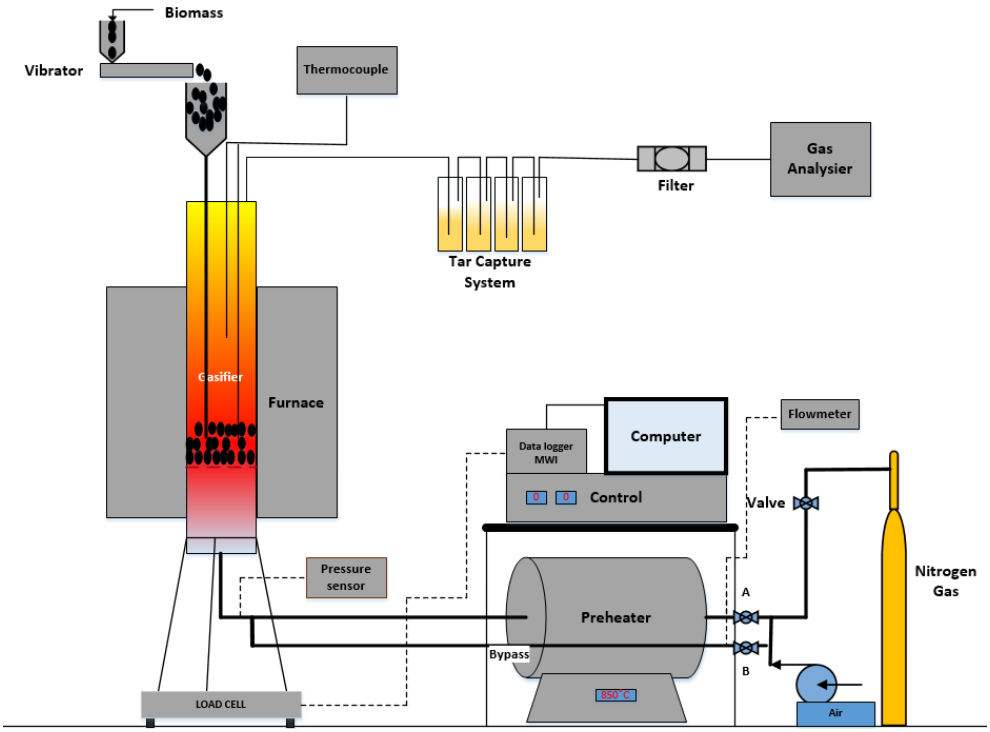

Figure 1. Thermogravimetric fluidized bed reactor (TGFBR).

During the pyrolysis and gasification experiments, a bed of silica sand weighing 400 g and having a density of 2650 kg/m^3 was used in the gasifier. The particle size of the sand was 500-600 µm. The height of the static bed was maintained at Hs=0.5D, meaning that half of the height was occupied by the bed material and the remaining half was the freeboard. The freeboard refers to the vertical distance separating the upper surface of the bed material from the termination point of the cylindrical tube. In order to avoid the escape of fluidized particles, it is necessary for the height of the freeboard to be no less than the Transport Disengaging Height (TDH), a crucial measurement for the fluidized bed column. [Al-Farraji, 2017, Yang, 2003]. For example, the TDH at $2U_{mf}$ (40 l/min) and the superficial gas velocity was 0.578 m.

2.1 Pyrolysis Test

The laboratory testing commenced by heating the fluidized bed reactor to the target temperature, while ensuring a consistent fluidization rate of the silica sand particles. After achieving the target temperature, the airflow was deactivated and the nitrogen flow rate was adjusted to double the minimum fluidization velocity (Umf). The nitrogen velocity was chosen based on two criteria: first, it allowed enough time for the reactor to reach a stable temperature; second, it was the lowest gas velocity needed to reduce external diffusion. For each test, a biomass amount of 40 g was used, which corresponded to 10% of the total weight of the bed material. The weight variation in the Two-Fluidized Bed Gasification Reactor (TGFBR) was monitored at one-second intervals during pyrolysis using a multifunction weight indicator model DFW06XP connected to the computer. The product gas was analyzed using a gas analyzer after passing through the tar cleaning unit. Nitrogen was used to maintain fluidization conditions and create an inert atmosphere, thereby preventing the oxidation of volatile products formed during the test. The

pyrolysis occurred at a high heating rate with a temperature range of 350 to 600°C, increasing in increments of 50°C.

2.2 Gasification Test

The experiment commenced once the appropriate temperature and steady-state conditions were achieved within the gasifier, ensuring that the silica sand particles maintained a consistent state of fluidization in conjunction with the air. The laboratory extraction system was initiated, and the suction pump was activated to divert a portion of the product gases to the gas analyzer. The feeder was triggered to provide a steady stream of biomass with a specific ER (Equivalence Ratio) into the gasifier, while the split furnace was deactivated directly. During the gasification trials, the heat produced was dissipated by utilizing ambient air. This was achieved by opening valve B and closing valve A, as depicted in Figure 1. Once the product gas underwent purification in the tar capture unit, the suction pump conveyed the gas to the gas analyzer. The gas analyzer continuously measured the volume concentration of gases throughout time. Following the shutdown of the gasifier, a cooling interval of 5 hours was observed until it reached room temperature. Subsequently, the sand was replenished in preparation for the next test. The gas analyzer underwent a process of purging using nitrogen gas and thereafter underwent recalibration. In order to avoid any obstructions caused by the elevated tar concentration during the gasification procedure, the PVC tubes employed for transferring the product gas from the gasifier to the analyzer were substituted with new pipes after each operation, while the stainless-steel pipes were subjected to cleaning.

The carbon conversion (ηc), cold gas efficiency (η), and higher heating value of dry gas (HHV) were used to determine the ERs and the effectiveness of the gasification process. The method for calculating these parameters was described in prior research. [Al-Farraji, 2017].

2.3 Kinetic Methods

The kinetic parameters of biomass pyrolysis in TGFBR were determined using a model-fitting method commonly employed for gas-solid reactions. The mechanism of the reaction was obtained by taking the derivative of the equations under isothermal conditions, as described in previous publications [Al-Farraji, 2017].

The TGFBR employed the integral model fitting method to estimate the kinetic parameters for isothermal methods.

$$G(x)=k(T)t \quad (1)$$

The term G(X) represents different integral model equations derived from Table 2, which can be utilized in Eq. (1). To evaluate the reaction expression using a reaction equation model, the linearity and linear range of G(X) are assessed at various temperatures against t. The rate constant at different temperatures is determined using the most appropriate model as shown in Eq. (2).

Taking the logarithm of the Arrhenius Equation, we obtain:

$$\ln k(T)=\ln(A)-E/RT \quad (2)$$

At multiple fixed temperatures, the experiments were conducted, and the activation energy was calculated using the Arrhenius equation, which involved plotting lnk versus 1/T (where T is the absolute temperature) and calculating the slope of the resulting graph.

Table 2. *Typical reaction Mechansim for hetrogeneous solid-state reaction.*

Symbol	*Reaction mechanism*	*f(x)*	G(x)
G1	One- dimensional diffusion, 1D	$1/2x$	x^2
G2	*Two- dimensional diffusion, (Valensi)*	$[-\ln(1-x)]^{-1}$	$x+(1-x)\ln(1-x)$
G3	*Three-dimensional diffusion, (Jander)*	$1.5(1-x)^{2/3}[1-(1-x)^{1/3}]^{-1}$	$[1-(1-x)^{1/3}]^2$
G4	*Three-dimensional diffusion, (G-B)*	$1.5[1-(1-x)^{1/3}]^{-1}$	$1-2x/3-(1-x)^{2/3}$
G5	*Three-dimensional diffusion(A-J)*	$1.5(1+x)^{2/3}[(1+x)^{1/3}-1]^{-1}$	$[(1+x)^{1/3}-1]^2$
G6	*Nucleation and growth(n=2/3)*	$1.5(1-x)[-\ln(1-x)]^{1/3}$	$[-\ln(1-x)]^{2/3}$
G7	*Nucleation and growth (n=1/2)*	$2(1-x)[-\ln(1-x)]^{1/2}$	$[-\ln(1-x)]^{1/2}$
G8	*Nucleation and growth (n=1/3)*	$3(1-x)[-\ln(1-x)]^{2/3}$	$[-\ln(1-x)]^{1/3}$
G9	*Nucleation and growth(n=1/4)*	$4(1-x)[-\ln(1-x)]^{1/3}$	$[-\ln(1-x)]^{1/4}$
G10	Autocatalytic reaction	$x(1-x)$	$\ln[x/(1-x)]$
G11	*Mampel power law(n=1/2)*	$2x^{1/2}$	$x^{1/2}$
G12	*Mampel power law(n=1/3)*	$3x^{2/3}$	$x^{1/3}$
G13	*Mampel power law(n=1/4)*	$4x^{3/4}$	$x^{1/4}$
G14	*Chemical reaction(n=3)*	$(1-x)^3$	$*[(1-x)^{-2}-1]/2*$
G15	*Chemical reaction(n=2)*	$(1-x)^2$	$*(1-x)^{-1}-1*$
G16	*Chemical reaction(n=1)*	$1-x$	*-ln(1-x)*
G17	*Chemical reaction(n=0)*	1	x
G18	*Contraction sphere*	$3(1-x)^{2/3}$	$1-(1-x)^{1/3}$
G19	Contraction cylinder	$2(1-x)^{1/2}$	$1-(1-x)^{1/2}$
Note: A-J: Anti- Jander; G-B: Ginstling-Brounshtein			

3. Results and Discussion

3.1 Pyrolysis Results

3.1.1 Influence of superficial gas velocity on total mass conversion rate

Figure 2 depicts the relationship between the conversion of total mass and the time it takes for a reaction to occur. This correlation is observed at different gas velocities that are lower than the maximum velocity at which silica sand particles settle. With an increase in the flow rate, the overall reaction time dropped. Specifically, at a flow rate of 0.123 m/sec, the reaction time was reduced to 63 seconds, compared to 278 seconds at a flow rate of 0.061 m/sec (equivalent to 20 liters per minute), while maintaining an operating temperature of 450°C. The reaction rate was determined by the gradient of the curve, which becomes less discernible beyond this threshold, even with a subsequent augmentation in the flow rate. Thus, this specific flow rate corresponds to the gas velocity that optimizes the response rate and greatly mitigates external diffusion constraints. [Xu, 2010]. To mitigate any impact of external diffusion on the reported rate, numerous researchers conduct initial thermogravimetric studies at different gas flow rates until no such influence is observed. [Gómez-Barea, 2005]. To prevent external diffusion, a superficial velocity of 0.123 m/sec was used for all experimental work, as it met the minimal gas velocity requirement.

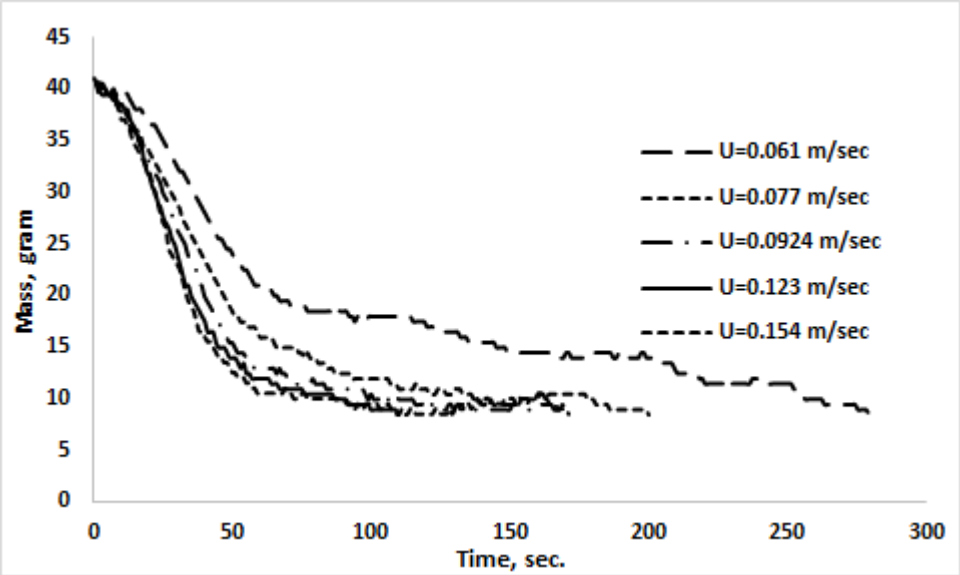

Figure 2: *Total mass conversion versus reaction time in TGFBR at different flow rates.*

3.1.2 Gas evolved varying with fluidized bed temperature.

Pyrolysis is a crucial step in the gasification of biomass in a fluidized bed reactor, and as such, the results of pyrolysis experiments can be beneficial in the advancement of lab and pilot-scale fluidized bed gasification processes. In a study involving palm stones, experiments were conducted at various temperatures ranging from 350°C to 750°C in 50°C increments to obtain valuable information. The pyrolysis of palm stones in a fluidized bed reactor produced CO, CO_2, CH_4, and H_2 gas products at different reaction temperatures and 2Umf velocity.

Figure 3 illustrates the correlation between reaction temperature and the concentration of product gas. No detection of methane and hydrogen occurred at temperatures below 500°C. However, the percentage of their volume started to rise above this temperature and peaked at around 750°C. Methane is generated through the thermal decomposition of tar at elevated temperatures. [Gai, 2015]. Nevertheless, as the temperature of the reactor is above 700°C, the degradation of CH4 also escalates. The increase in the production of the primary gaseous products at elevated temperatures is mostly due to the subsequent decomposition of the pyrolysis vapours [Xianwen, 2000, Horne, 1996]. The production of carbon monoxide (CO) exhibited a consistent upward trend as the reaction temperature increased, reaching its highest point at 14.93% when the temperature reached 750°C. The CO2 volume exhibited a positive correlation with temperature, reaching its peak at 500°C, followed by a marginal decline at 550°C. Starting at a temperature of 550°C, the volume of CO2 remained consistently stable. At temperatures below 550°C, the amount of carbon monoxide (CO) generated was lower than the amount of carbon dioxide (CO2) produced. However, at temperatures over 550°C, the amount of carbon monoxide surpassed the amount of carbon dioxide.

The results indicate that as temperature increases, CO production also increases. The elevated temperatures within the gasifier encourage cracking reactions, resulting in a rise in the concentration of CO. A comparison with literature showed that biomass pyrolysis in a micro fluidized bed yielded CO_2 at low temperatures, suggesting that carboxyl reactions may occur more easily. However, at temperatures ranging from 600-900°C, the concentration of CO_2 remains constant and low, suggesting complete decomposition of carboxyl or ester functional groups at temperatures above 600°C. [Yang, 2007, Jian, 2010]. The current investigation has also observed similar patterns, where all the components of the product gas showed distinct variations in the order and duration of their release at two different temperatures, specifically 350°C and 600°C, as depicted in Figure 4. It can be shown that at a temperature of 350°C, a greater amount of CO2 was emitted compared to CO at the start of the time period. At a temperature of 600°C, there was a shift in the condition, with the release of carbon monoxide surpassing that of carbon dioxide. Prior research has indicated that higher pyrolysis temperatures promote the thermal breakdown of

hydrocarbons in gaseous products. This results in an elevated production of hydrogen and carbon monoxide, while reducing the amount of carbon dioxide present [Vigouroux, 2001]. The present investigation detected variations in the release sequence and duration of the product gas components at two distinct temperatures, specifically 350°C and 600°C, as depicted in Figure 4. At 350°C, CO_2 was released more quickly than CO. However, at 600°C, the release of CO exceeded that of CO_2. This finding is consistent with previous research that suggested that high pyrolysis temperatures favour the thermal decomposition of hydrocarbons in the gas products, leading to increased yields of hydrogen and CO and reduced CO_2 content.

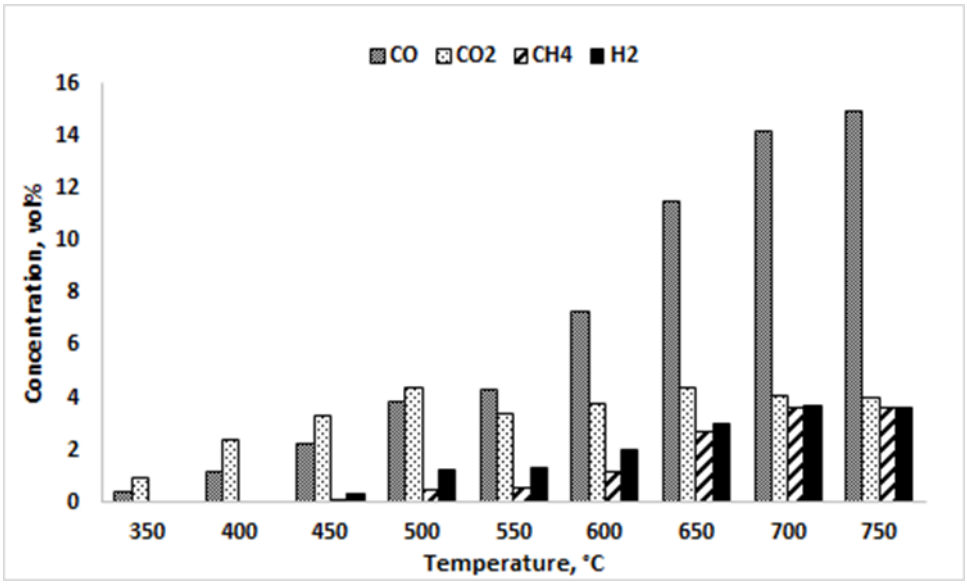

Figure 3. Effect of temperature on gas product from pyrolysis of palm stones.

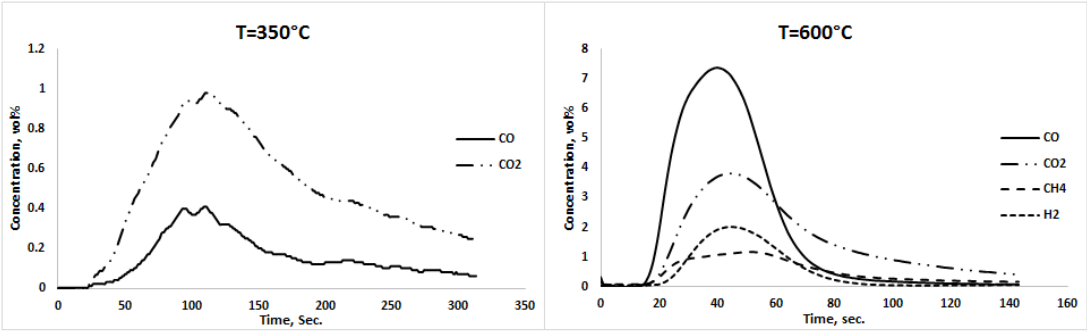

Figure 4. Evolved major gas species of palm stones and their release sequences during pyrolysis.

3.1.3 Impact of bed temperature on overall conversion rate

Figure 5 illustrates the correlation between the overall conversion of palm stone and temperature. The graph illustrates the main conversion reaction, predominantly caused by the thermal degradation of biomass into volatile substances and char. Temperature changes that arise throughout the reaction have a substantial impact on the advancement of reactions in pyrolysis. During a fluidized bed fast pyrolysis process, the feedstock particles are subjected to an exceptionally intense heat flux, leading to a rapid increase in temperature. Scientists have proven that the highest amounts of liquids may be produced by using fast heating rates and temperatures of approximately 500°C [Chhiti, 2013]. The results of the experiments indicated that at temperatures of 500°C and above, there were high levels of conversion, which were measured based on mass loss. At a temperature of 500°C, the conversion rate was around 90% and took less than 45 seconds. Increasing the temperature did not significantly affect this value, indicating that the pyrolysis process of palm stones was operating under fast pyrolysis conditions.

This is in agreement with Bridgwater et al. [2000], The fast pyrolysis process has a key attribute whereby it can produce yields up to 80% of the dry feed. The quick breakdown of palm stones at high temperatures, as indicated by the conversion figure, is due to the high amount of volatile matter and low ash content in the date stones, as shown in Table 1 of the proximate analysis. This finding is consistent with the research of Munir et al. [2009]. Conversely, at temperatures exceeding 500°C, the thermal decomposition of heavy hydrocarbons (tar) resulted in an increase in combustible gases during pyrolysis, as depicted in Figure 3. The production of significant gas components from tar during thermal cracking is influenced by the reaction temperature, which is a crucial factor in determining gas formation [Gai, 2015]. This finding aligns with the observation made by Yu et al. [2010] hat high temperature pyrolysis yields a greater amount of non-condensable gases and a lesser amount of tar. Encinar et al. [1998] observed that with an increase in reactor temperature, the quantity of liquid generated during the pyrolysis of olive bagasse reduced, while the gas production rose. This suggests that the increase in gas production is partially attributed to the vigorous fragmentation of liquid under elevated temperatures. To investigate the kinetic data of palm stones, a temperature range of 350 to 600°C was used.

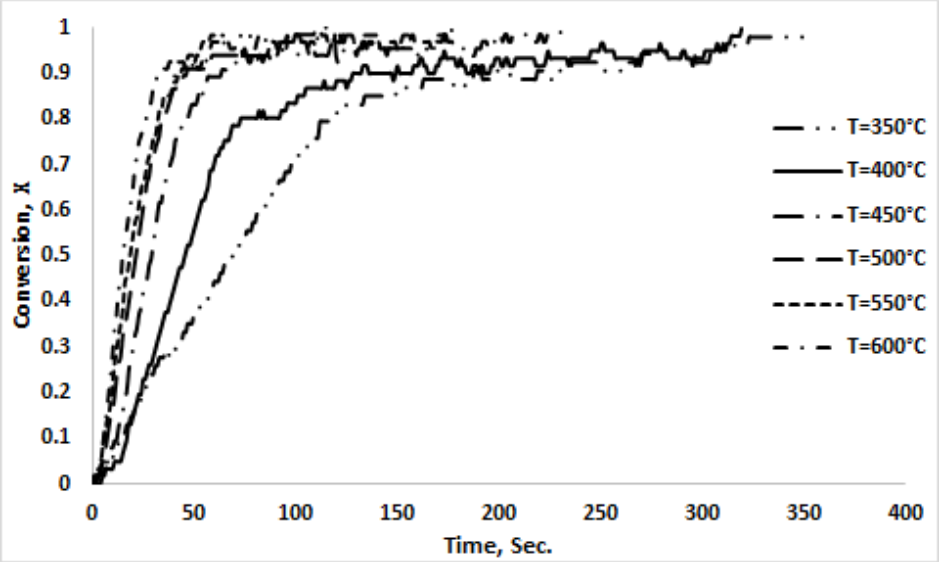

Figure 5: *Conversion vs reaction time in fluidized bed reactor at different temperatures.*

3.1.4 Char yield of palm stones during pyrolysis

The thermal decomposition of the biomass in the absence of oxygen produces solids in the form of char, liquids and gases [Yaman, 2004]. To determine the amount of char produced during the pyrolysis test, the laboratory scale was used to weigh the palm stones fed into the fluidized bed. The load cell attached to the reactor was used to measure the resulting char. Therefore, the mass of char collected represents the actual amount of char in the reactor, indicating that no additional secondary reaction took place. All yields were calculated on a dry basis, and the experimental error of ±0.5 wt% was obtained by averaging the yield from three separate experiments.

The impact of bed temperature on char yield as a percentage of dry date palm stone is displayed in Figure 6, showing a decrease from 34 wt% at 350°C to 16 wt% at 600°C. A significant decline in char yield of 27 wt% occurred between 350°C and 500°C, after which the yield remained stable. Biomass mainly comprises hemicellulose, cellulose, and lignin, which are decomposed at temperatures of 260-340°C, 320-380°C, and 300-580°C, respectively. The abrupt decrease in char yield below 500°C is caused by the breakdown of hemicellulose and cellulose. However, at temperatures above 500°C, the mass loss is negligible, as reported by Al-Farraji et al. in 2017, The decomposition rate slows at higher temperatures due to the breakdown of lignin, which occurs above 380°C during the pyrolysis of olive kernels. In contrast, the thermal behaviour of date palm stones was examined using thermo-gravimetric analysis (TGA), and the findings showed that thermal decomposition was completed at temperatures below 500°C

[Nasser, 2016]. It is apparent that as the temperature rises, both the char yield and time conversion decrease. This means that less char is produced in a shorter period at higher temperatures [Solís, 2016], see Figure 5.

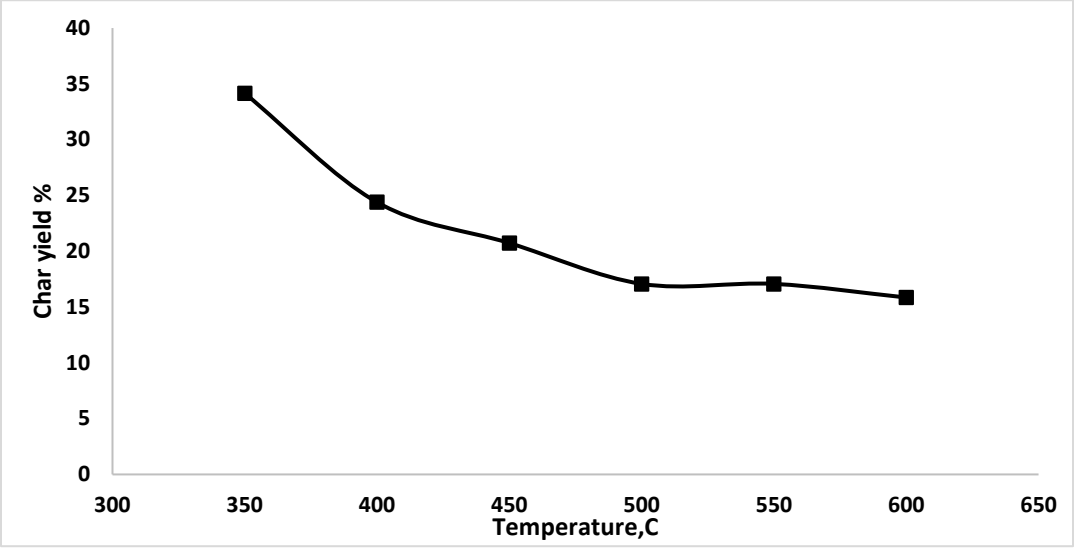

Figure 6. *Effect of temperature on char yield.*

3.1.5 Kinetic Parameters

Continuous measurements of palm stone weight were conducted during pyrolysis in order to determine the biomass conversion at six distinct temperatures, ranging from 350°C to 600°C. The pyrolysis of palm stones in a fluidized bed reactor, conducted under isothermal circumstances, is a heterogeneous reaction that may be examined using a universal integral technique to ascertain the most probable reaction pathways.

Equation (1) can be employed to establish a correlation between G(x) and t at a certain reaction temperature. This correlation can be represented by a straight line, where the slope corresponds to k(t). Several solid-state mechanism models (as indicated in Table 2) were evaluated in order to identify an appropriate match. Five potential response models were chosen based on the fitting correlation coefficient (R2) quality. The graphs depicting these models may be observed in Figures 7 and 8.

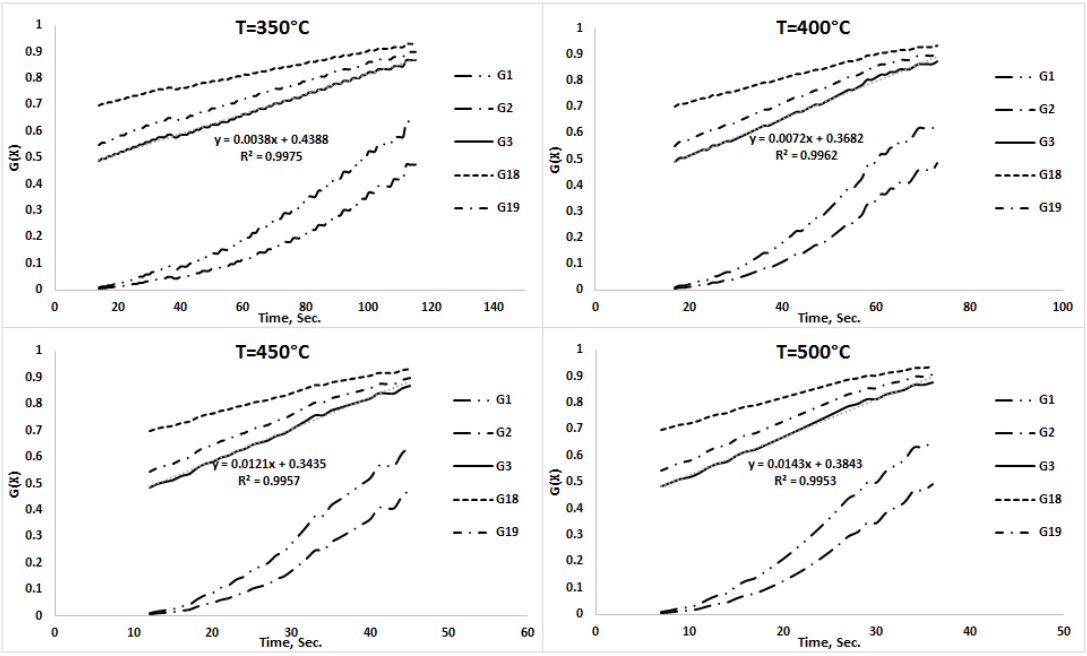

***Figure 7**. Correlation of G(x) versus time at temperatures 350, 400, 450, and 500°C for palm stones.*

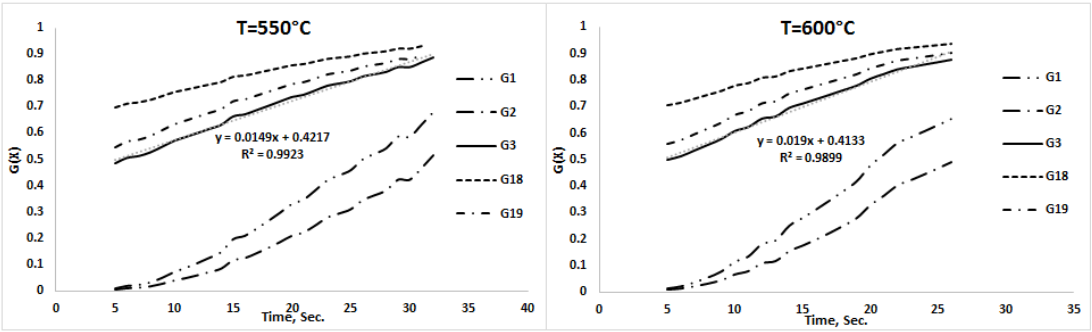

Figure 8. Correlation of G(x) versus time at temperatures 550 and 600°C.

Table 3 displays the kinetic parameters and fitting correlation coefficients (R2) for the five major models. The most probable reaction mechanism that could elucidate the thermal degradation of palm stones in the fluidized bed reactor is three-dimensional diffusion. This mechanism is linked to an increased breakdown of hemicellulose and cellulose, resulting in a higher volatility of the primary constituents of biomass in this temperature range. Poletto et al. identified comparable pathways in biomass [Poletto, 2012] as well as Wang et al. [2006].

Table 3. *Reaction model for palm stone decomposition during isothermal fluidized bed pyrolysis.*

G(x)	G1	G2	G3	G18	G19
Temp (°C)	350	350	350	350	350
R^2 (%)	96.84	94.07	99.75	99.72	99.72
ln k(T)	-5.051	-5.381	-5.572	-6.074	-5.683
Temp (°C)	400	400	400	400	400
R^2 (%)	97.54	95.40	99.62	99.43	99.43
ln k(T)	-4.390	-4.699	-4.933	-5.426	-5.035
Temp (°C)	450	450	450	450	450
R^2 (%)	98.05	96.10	99.57	99.18	99.18
ln k(T)	-3.892	-4.213	-4.414	-4.919	-4.509
Temp (°C)	500	500	500	500	500
R^2 (%)	97.94	95.98	99.53	99.16	99.16
ln k(T)	-3.709	-4.011	-4.247	-4.744	-4.342
Temp (°C)	550	550	550	550	550
R^2 (%)	98.96	97.21	99.23	98.52	98.52
ln k(T)	-3.661	-3.963	-4.206	-4.688	-4.290
Temp (°C)	600	600	600	600	600
R^2 (%)	98.91	97.64	98.99	98.27	98.27
ln k(T)	-3.411	-3.684	-3.963	-4.474	-4.068

A logarithmic representation of the rate constant, k, was plotted against the reciprocal of the temperature, 1/T, resulting in an Arrhenius plot (see Figure 9). The activation energy for the pyrolysis tests of palm stones was calculated to be 27.67 kJ/mole by calculating the slope of (-Ea/R) from the lnk against 1/T plots. The temperatures ranged from 350°C to 600°C. The activation energy for non-isothermal circumstances was found to be 30.7 kJ/mole using a TGA [Sait, 2012]. The larger activation energy (Ea) seen in the thermogravimetric analysis (TGA) can be explained by the lower heating rate used in TGA compared to the fluidized bed reactor. Additionally, the gas diffusion inhibition in TGA also contributes to the higher Ea. These observations are consistent with the findings reported by Yu et al. [2011]. The findings derived from the kinetic analysis of palm stone pyrolysis, in conjunction with the elucidation of transport processes, can offer significant insights for the development and enhancement of the thermochemical process.

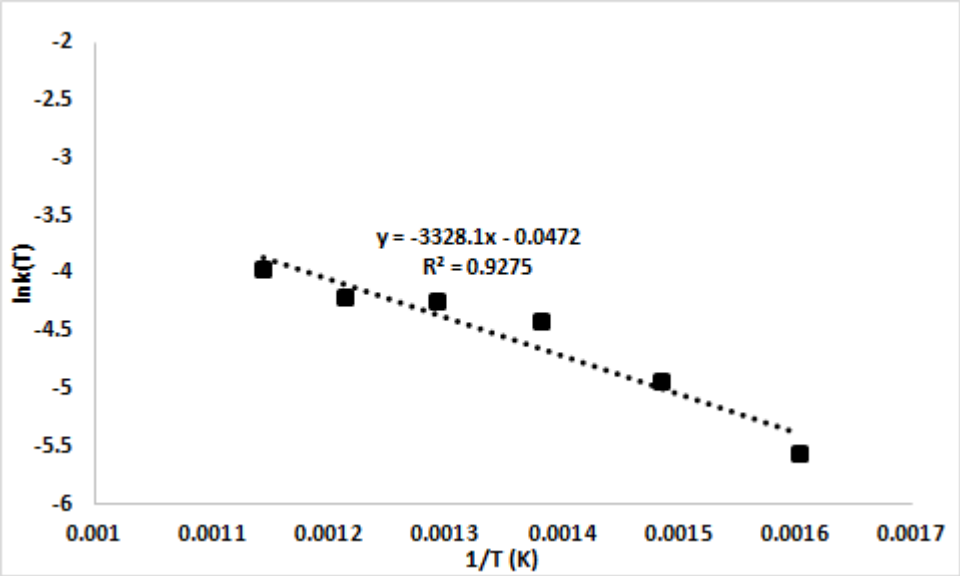

Figure 9. Kinetic plots for palm stones pyrolysis.

3.2 Gasification results

This study examined the gasification performance of palm stones over a range of temperatures from 600 to 750°C and equivalence ratios between 0.15 and 0.35 to determine the best conditions. The subsequent sections will explore the results of this investigation.

3.2.1 Effect of different bed temperatures on the product gases.

The temperature of the bed plays a significant role in the combustion and gasification reactions. To investigate this, the current study varied the bed temperature from 600 to 750°C in increments of 50°C at an equivalence ratio of 0.2. The findings of this experimentation are displayed in Figure 10.a and Table 4.

The study's results demonstrate a positive correlation between bed temperature and the concentrations of CO, H2, and CH4. The concentrations of CO range from 11.97 to 17.54 vol%, H2 ranges from 3.11 to 5.5 vol%, and CH4 ranges from 3.22 to 5.01 vol%. Le Chatelier's principle states that elevated temperatures enhance the presence of reactants in exothermic reactions, while promoting the formation of products in endothermic processes. Increasing the temperature enhances the endothermic reaction, leading to the production of H2 gas by increasing the breakdown of tar in the early stage and facilitating the water-gas reaction [Skoulou, 2009]. Additionally, the water-gas reaction R3 is promoted. The water-gas reaction can take place in any gasifier, regardless of the presence of water only in the biomass. The water vapor present in the air supplied to the gasifier can also participate in this reaction. As stated by Cao et al. [2006]. The gasification of biomass is enhanced by the presence of water vapor and CO2, which encourage the production of H_2. As temperature increases, the concentration of CO also rises due to R1 (as shown in Fig. 3), R4, and R10. On the other hand, the concentration of CO_2 decreases as the temperature rises, while the CO concentration rises. The heat necessary to maintain the reaction mainly originates from the oxidation process. The CO_2 produced may have been utilized by tar cracking and Boudouard reactions, resulting in a decrease in CO_2 concentration at the higher temperatures studied [Almeida, 2015]. At a temperature of 600°C, the CO_2 level was measured at 15.03%, which decreased to 13.18% when the temperature was increased to 750°C. The process of tar cracking to CH_4, H_2, and CO at high temperatures can cause the production of methane [Lahijani, 2011]. Esfahani has supported this claim by stating that the rise in gas concentration as the temperature increases can be attributed to several factors, such as (i) faster gas production during the initial pyrolysis stage at higher temperatures, (ii) favourable endothermic char gasification reactions at higher temperatures resulting in more gas production, and (iii) increased gas yield due to the cracking of heavier hydrocarbons and tars as a consequence of higher temperatures [Esfahani, 2012].

Table 4 displays the findings on the fluctuations in cold gas efficiency, carbon conversion efficiency, gas yield, and HHV (higher heating value). The process attained its highest carbon conversion and cold gas efficiency at a temperature of 750°C, hitting 56.3% and 34.47% respectively. The increase in carbon conversion efficiency was attributed to an augmentation in the oxidation reaction, resulting in a higher yield of combustible gases and thus enhancing the cold gas efficiency.

As anticipated, raising the temperature of the bed led to an augmentation in gas production, possibly attributed to enhanced thermal degradation of liquids and heightened interaction between the char and the gasification agent. The gas yield increased from 1.25 m3/kg at a temperature of 600°C to 1.43 m3/kg at 750°C. The increase in temperatures resulted in a decrease in the production of char and tar, while simultaneously increasing the yield of gas by releasing a greater amount of volatile compounds [Ahmad, 2016]. At a temperature of 750°C, the higher heating value (HHV) was determined to be 4.91 MJ/m3. This value is attributed to the presence of combustible gases such as CO, H_2, and CH_4.

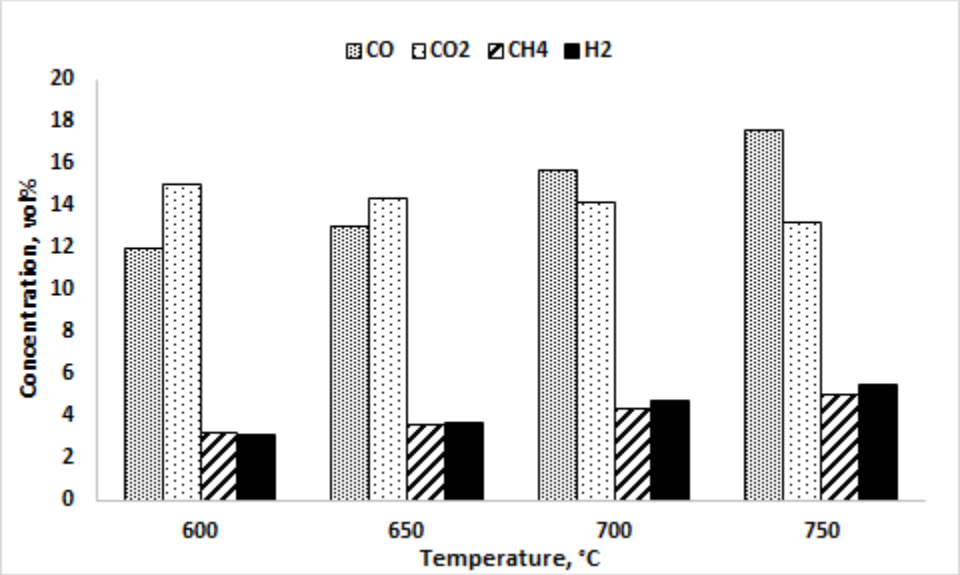

Figure 10*.a Effect of temperature on gas composition of palm stones at ER=0.2.*

Table 4. *Summary of results for application of different gasification temperatures of palm stones.*

Temperature °C	**600**	**650**	**700**	**750**
Gas yield (m^3/kg)	1.25	1.28	1.37	1.43
Carbon conversion efficiency (%)	41.83	43.67	51.7	56.3
Cold gas efficiency (%)	19.67	22.19	29.1	34.47
HHV (MJ/Nm^3)	3.19	3.53	4.31	4.91

3.2.2 Influence of equivalence ratio (ER).

In order to investigate the effect of equivalence ratio (ER) on gasification performance, the ER was varied between 0.15 and 0.35 while the bed temperature was kept constant at 750°C, with the air flow rate remaining constant and the mass flow rate of biomass being changed accordingly to minimize the impact on gas residence time. Table 5 shows the results of the test. As can be seen in Figure 10.b, the formation of CO, CO_2, H_2, and CH_4 increased slightly as the ER increased from 0.15 to 0.2. Nevertheless, with a further rise in the ER to 0.35, the generation of CO, CH4, and H2 declined, while the creation of CO2 escalated. This occurs due to the direct relationship between raising the equivalence ratio (ER) and the air flow rate, which subsequently enhances the combustion process and promotes the char oxidation reaction. Consequently, this results to a higher production of carbon dioxide (CO2) while depleting combustible gases like carbon monoxide (CO), methane (CH4), and hydrogen (H2). Under conditions of low equilibrium ratio (ER), carbon monoxide (CO), methane (CH4), and hydrogen (H2) were generated through the thermal breakdown of carbonaceous material. The formation of carbon monoxide (CO) was more favorable compared to carbon dioxide (CO2) due to the limited availability of oxygen. Nevertheless, as the ERs increased, the combustion reaction took precedence, resulting in a decline in the formation of CO, CH4, and H2, and a rise in CO2. More precisely, the concentrations of carbon monoxide (CO), methane (CH4), and hydrogen (H2) fell from 17.54%, 5.01%, and 5.5% respectively at an equivalence ratio (ER) of 0.2 to 9.03%, 2.4%, and 2.75% respectively at an ER of 0.35. On the other hand, the concentration of carbon dioxide (CO2) increased from 13.18% to 15.45%. Skoulou concurred with this [Skoulou, 2008], who stated, Altering the ER during gasification may result in reaching either of two opposite operating conditions: one where the gasification proceeds entirely towards CO, and the other where complete combustion results in CO_2

Table 5 and Figure 10.c illustrate the relationship between gasification performance and the equivalence ratio (ER) in terms of higher heating value (HHV), energy yield, cold gas efficiency, and gas yield. The energy yield (MJ/kg biomass) of these five tests is determined by the gas yield (Nm3/kg biomass) and the higher heating value (HHV) (MJ/m3). The gas production rose from 1.07 Nm3/kg at an equivalent ratio (ER) of 0.15 to 2.09 Nm3/kg within the range of equivalence ratios examined. The increase in gas production is related to the elevated concentration of nitrogen (N2) in the gas yield. At an ER (equivalence ratio) of 0.35, the gas production was at its peak, but its HHV (higher heating value) was the lowest, measuring 2.44 MJ/m3. This was caused by the increased oxidation processes of the combustible gases [Lv, 2004]. The carbon conversion efficiency had a positive correlation with the ER, reaching its peak value at ER=0.3.

The results suggest that increasing the ER values to 0.15 and 0.2 had a positive effect on both HHV and cold gas efficiency. Specifically, HHV increased from 4.78 to 4.9 MJ/m3, and cold gas efficiency increased from 25.09% to 34.47%. The rise in the product gas can be ascribed to the higher concentration of flammable gases.

The gasification of palm stone was compared to the results reported in other studies that investigated the gasification of different types of biomass. In this study, the cold gas efficiency and higher heating value (HHV) were observed to be lower compared to a previous study on palm empty fruit bunch gasification. The previous study utilized an air-blown fluidized bed at a temperature of 770°C, resulting in a cold gas efficiency of 40% and HHV of 4.53 MJ/m^3 [Lahijani, 2011]. In a study conducted by Kim et al. [2013], wood pellets were gasified using biomass in an air-blown fluidized bed reactor. The biomass was fed into the gasifier from the top. The results indicated that as the equivalence ratio (ER) decreased from 0.27 to 0.19, the concentration of syngas increased. The produced gas achieved a maximum calorific value of 4.7 MJ/Nm^3.

Based on the analysis of experimental data at various ER values, it can be concluded that using too small or too large ER values is not feasible for biomass gasification. A low ER value leads to a lower reaction temperature, which increases the amount of tar produced and is unfavourable for palm stone gasification. On the other hand, using a high ER value leads to the consumption of more combustible gases through oxidation reactions. Therefore, in the current study, the optimal ER value was found to be 0.2 under the conditions listed in Table 5. At this value, the energy yield of product gas was found to be 7 MJ/kg biomass with a standard deviation error of 0.45%.

***Table 5**. Summary of results for the application of different ER in palm stones gasification.*

ER	0.15	0.2	0.25	0.3	0.35
Biomass flow rate dry basis (kg/hr)	3.11	2.33	1.86	1.55	1.33
Air flow rate (Ndm^3/min)	40	40	40	40	40
Temperature, °C	750	750	750	750	750
Gas yield (Nm^3/kg)	1.07	1.43	1.64	1.88	2.09
Cold gas efficiency (η)	25.09	34.47	30.52	29.12	25.14
Energy yield (MJ/kg)	5.11	7.0	6.18	5.92	5.09

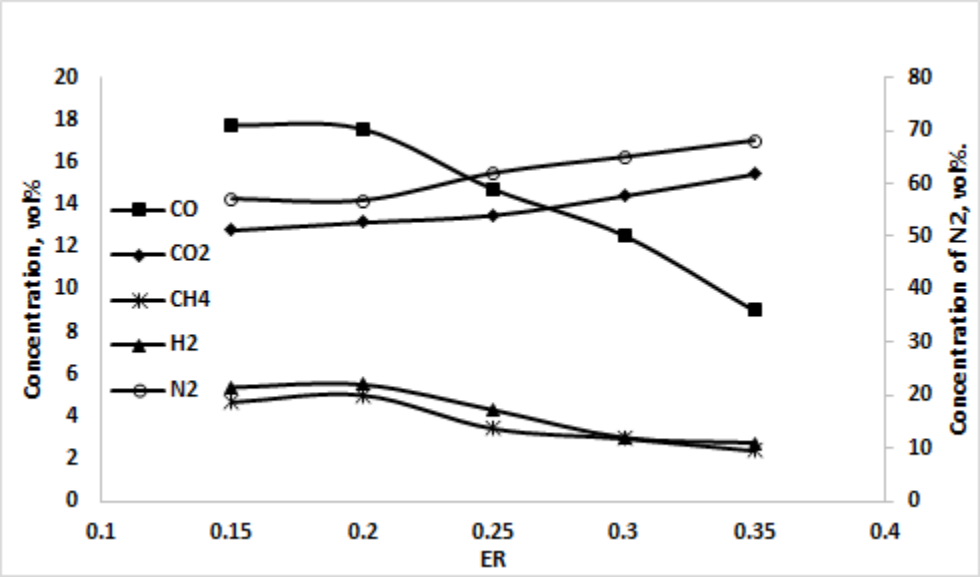

***Figure 11**. Influence of ER on gas composition for palm stone gasification at 750C.*

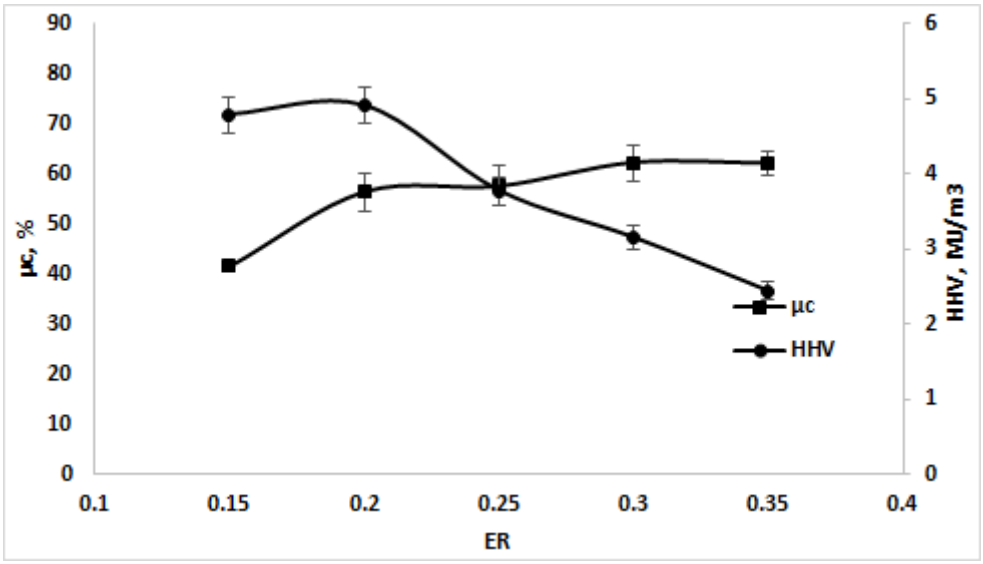

Figure 12 *Influence of ERs on the HHV and carbon efficiency during date palm stone gasification.*

4. Conclusions

Palm stones are a fascinating form of biomass due to their abundance as agricultural residue. A bubbling fluidized bed reactor was used to perform fast pyrolysis on them. The minimum superficial velocity required to minimize external diffusion during pyrolysis was found to be $2U_{mf}$, which varied depending on the specific velocity used.

The temperature of the pyrolysis bed was found to have a significant impact on both the total conversion of biomass and the resulting product gas. CH_4 and H_2 gases were not generated below 500°C, but their production increased with higher temperatures due to more thermal decomposition of larger hydrocarbons. CO_2 formation also increased with temperature, but after 550°C, it became less sensitive to temperature. On the other hand, CO concentration increased with temperature and peaked at 750°C. Experimental results indicated a high level of conversion based on mass loss when the temperature was 500°C or higher.

Using a model-fitting approach, the kinetic parameters for the pyrolysis of palm stone were assessed, revealing an activation energy of 27.67 kJ/mole and a three-dimensional diffusion mechanism for the reaction. The kinetic parameters obtained from this study, such as the activation energy, are crucial for scaling up effective conversion technologies like pyrolysis.

In the gasification of palm stones using a bubbling fluidized bed gasifier, both temperature and equivalence ratio had a significant impact on the distribution of gases produced. Higher temperatures led to greater production of combustible gases and reduced formation of CO_2, as well as improved carbon conversion and cold gas efficiency. A low equivalence ratio was preferable based on the investigation of this parameter. The study identified the optimal conditions for palm stones gasification as T=750°C and ER=0.2, producing a maximum HHV of 4.9 (MJ/m^3), which is suitable for use in internal combustion engines. Future efforts to improve HHV could involve adding a catalyst to the gasifier to enhance tar cracking and increase the yield of combustible gases.

4.1 Symbols Used

Greek letters

Symbol	Unit	Definition/explanation
η	-	Cold gas efficiency
ηc		Carbon conversion

Sub- and Superscripts

Symbol	Unit	Definition/explanation
mf	-	Minimum fluidized
s		Static bed

Abbreviations

Symbol	Unit	Definition/explanation
ER	-	Equivalence ratio
G(x)	M^3/kg	Gas yield for gas x
HHV	MJ/Nm^3	Higher heating value
H_s	m	Static bed height
TDH	m	Transport disengaging height
TGA	-	Thermogravimetric analysis
TGFMR	-	Thermal-gravimetric fluidized bed reactor
U_{mf}	m/s	Minimum fluidization velocity

References

[1] Abdoulmoumine N., Kulkarni A., and Adhikari S., (2014) Effects of temperature and equivalence ratio on pine syngas primary gases and contaminants in a bench-scale fluidized bed gasifier, *Industrial & Engineering Chemistry Research* vol. 53, no. 14, pp. 5767-5777, 2014.

[2] Ahmad A. A., Zawawi N. A., Kasim F. H., Inayat A., and Khasri A., (2016) Assessing the gasification performance of biomass: A review on biomass gasification process conditions, optimization and economic evaluation, *Renewable and Sustainable Energy Reviews* vol. 53, pp. 1333-1347, 2016.

[3] Ahmed J. M. R. H. S. and Mossa H. A., (2011) Analysis of Troposphere Carbon Dioxide in IRAQ from Atmosphere Infrared Sounder (AIRS) data: 2011.

[4] Al-Aasadi K. A., Alwaeli A. A., and Kazem H. A., (2015) Assessment of Air Pollution caused by Oil Investments in Basra Province-Iraq, *J Nat Academ Sci* vol. 4, no. 1, pp. 82-86, 2015.

[5] Al-Farraji A. (2017) Chemical Engineering and Reactor Design of a Fluidised Bed Gasifier, PhD, School of Engineering-Cardiff University Cardiff, United Kingdom, 2017. [Online]. Available: https://orca.cardiff.ac.uk/id/eprint/104985

[6] Al-Farraji A., Marsh R., and Steer J., (2017) A Comparison of the Pyrolysis of Olive Kernel Biomass in Fluidised and Fixed Bed Conditions, *Waste and Biomass Valorization,* journal vol. 8, no. 4, pp. 1273-1284, June 01 2017, DOI: 10.1007/s12649-016-9670-6.
[7] Al-Farraji A., Marsh R., Steer J., and Valera-Medina A., (2017) Kinetics and Performance of Raw and Torrefied Biomass in a Continuous Bubbling Fluidized Bed Gasifier, *Waste and Biomass Valorization journal* December 16 2017, doi: 10.1007/s12649-017-0167-8.
[8] Almeida A. *et al.*, (2015) Effect of temperature on the gasification of olive bagasse particles, in *6th International Congress of Energy and Environment Engineering and Management, Paris*, 2015.
[9] Bridgwater A. and Peacocke G. (2000) Fast pyrolysis processes for biomass, *Renewable and sustainable energy reviews* vol. 4, no. 1, pp. 1-73, 2000.
[10] Cao Y., Wang Y., Riley J. T., and Pan W.-P., (2006) A novel biomass air gasification process for producing tar-free higher heating value fuel gas, *Fuel Processing Technology* vol. 87, no. 4, pp. 343-353, 2006.
[11] Chhiti Y. and Kemiha M., (2013) Thermal Conversion of Biomass, Pyrolysis and Gasification, *International Journal of Engineering and Science (IJES)* vol. 2, no. 3, pp. 75-85, 2013.
[12] El-Juhany L. I., (2010) Degradation of date palm trees and date production in Arab countries: causes and potential rehabilitation, *Australian Journal of Basic and Applied Sciences* vol. 4, no. 8, pp. 3998-4010, 2010.
[13] Encinar J., Beltran F., Ramiro A., and Gonzalez J., (1998) Pyrolysis/gasification of agricultural residues by carbon dioxide in the presence of different additives: influence of variables, *Fuel Processing Technology* vol. 55, no. 3, pp. 219-233, 1998.
[14] Erskine W. *et al.*, (2004) Date palm in the GCC countries of the Arabian Peninsula, in *Proc. Regional Workshop on Date Palm Development in the Arabian Peninsula, Abu Dhabi, UAE*, 2004.
[15] Esfahani R. M., Wan A K G W. A., Mohd S M. A., and Ali S., (2012) Hydrogen-rich gas production from palm kernel shell by applying air gasification in fluidized bed reactor, *Energy & Fuels* vol. 26, no. 2, pp. 1185-1191, 2012.
[16] Gai C., Dong Y., Fan P., Zhang Z., Liang J., and Xu P., (2015) Kinetic study on thermal decomposition of toluene in a micro fluidized bed reactor, *Energy Conversion and Management* vol. 106, pp. 721-727, 2015.
[17] Gai C., Dong Y., Lv Z., Zhang Z., Liang J., and Liu Y., (2015) Pyrolysis behavior and kinetic study of phenol as tar model compound in micro fluidized bed reactor, *International Journal of Hydrogen Energy* vol. 40, no. 25, pp. 7956-7964, 2015.
[18] Gómez-Barea A., Ollero P., and Arjona R., (2005) Reaction-diffusion model of TGA gasification experiments for estimating diffusional effects, *Fuel* vol. 84, no. 12, pp. 1695-1704, 2005.
[19] Horne P. A. and Williams P. T., (1996) Influence of temperature on the products from the flash pyrolysis of biomass, *Fuel* vol. 75, no. 9, pp. 1051-1059, 1996.
[20] Jeguirim M., Bikai J., Elmay Y., Limousy L., and Njeugna E., (2014) Thermal characterization and pyrolysis kinetics of tropical biomass feedstocks for energy recovery, *Energy for Sustainable Development* vol. 23, pp. 188-193, 2014.
[21] Jian Y., ZHU J.-h., Feng G., DUAN Z.-k., LIU Y.-y., and XU G.-w., (2010) Reaction kinetics and mechanism of biomass pylolysis in a micro-fluidized bed reactor, *Journal of fuel chemistry and technology* vol. 38, no. 6, pp. 666-672, 2010.
[22] Kazem H. A. and Chaichan M. T., (2012) Status and future prospects of renewable energy in Iraq, *Renewable and Sustainable Energy Reviews* vol. 16, no. 8, pp. 6007-6012, 2012, doi: https://DOI.org/10.1016/j.rser.2012.03.058.
[23] Kim Y. D. *et al.*, (2013) Air-blown gasification of woody biomass in a bubbling fluidized bed gasifier, *Applied energy* vol. 112, pp. 414-420, 2013.
[24] Lahijani P. and Zainal Z. A., (2011) Gasification of palm empty fruit bunch in a bubbling fluidized bed: a performance and agglomeration study, *Bioresource Technology* vol. 102, no. 2, pp. 2068-2076, 2011.
[25] Lv P., Chang J., Wang T., Wu C., and Tsubaki N., (2004) A kinetic study on biomass fast catalytic pyrolysis, *Energy & fuels* vol. 18, no. 6, pp. 1865-1869, 2004.
[26] Lv P., Xiong Z., Chang J., Wu C., Chen Y., and Zhu J., (2004) An experimental study on biomass air–steam gasification in a fluidized bed, *Bioresource technology* vol. 95, no. 1, pp. 95-101, 2004.
[27] Munir S., Daood S., Nimmo W., Cunliffe A., and Gibbs B., (2009) Thermal analysis and devolatilization kinetics of cotton stalk, sugar cane bagasse and shea meal under nitrogen and air atmospheres, *Bioresource Technology* vol. 100, no. 3, pp. 1413-1418, 2009.
[28] Nasser R. A. *et al.*, (2016) Chemical analysis of different parts of date palm (Phoenix dactylifera L.) using ultimate, proximate and thermo-gravimetric techniques for energy production, *Energies* vol. 9, no. 5, p. 374, 2016.
[29] Poletto M., Zattera A. J., and Santana R. M., (2012) Thermal decomposition of wood: kinetics and degradation mechanisms, *Bioresource technology* vol. 126, pp. 7-12, 2012.
[30] Sait H. H., Hussain A., Salema A. A., and Ani F. N., (2012) Pyrolysis and combustion kinetics of date palm biomass using thermogravimetric analysis, *Bioresource Technology* vol. 118, pp. 382-389, 2012.
[31] Skoulou V., Swiderski A., Yang W., and Zabaniotou A., (2009) Process characteristics and products of olive kernel high temperature steam gasification (HTSG), *Bioresource technology* vol. 100, no. 8, pp. 2444-2451, 2009.
[32] Skoulou V., Zabaniotou A., Stavropoulos G., and Sakelaropoulos G., (2008) Syngas production from olive tree cuttings and olive kernels in a downdraft fixed-bed gasifier, *International Journal of Hydrogen Energy* vol. 33, no. 4, pp. 1185-1194, 2008.

[33] Solís H S., (2016) Biochar production by biomass pyrolysis for various applications, 2016.
[34] Vigouroux R. Z., (2001) Pyrolysis of biomass, *Royal Institute of Technology,* 2001.
[35] Wang J. *et al.*, (2006) A comparative study of thermolysis characteristics and kinetics of seaweeds and fir wood, *Process Biochemistry* vol. 41, no. 8, pp. 1883-1886, 2006.
[36] Xianwen D., Chuangzhi W., Haibin L., and Yong C., (2000) The fast pyrolysis of biomass in CFB reactor, *Energy & Fuels* vol. 14, no. 3, pp. 552-557, 2000.
[37] Xu G., Gao S., Yu J., Li Q., Zhu J., and Duan Z., (2010) Characteristics and kinetics of biomass pylolysis in a micro fluidized bed reactor, 2010
[38] Yaman S., (2004) Pyrolysis of biomass to produce fuels and chemical feedstocks, *Energy conversion and management* vol. 45, no. 5, pp. 651-671, 2004.
[39] Yang H., Yan R., Chen H., Lee D. H., and Zheng C., (2007) Characteristics of hemicellulose, cellulose and lignin pyrolysis, *Fuel* vol. 86, no. 12, pp. 1781-1788, 2007.
[40] Yang W.-c., (2003) *Handbook of fluidization and fluid-particle systems*. CRC press, 2003.
[41] Yu J. *et al.*, (2010) Kinetics and mechanism of solid reactions in a micro fluidized bed reactor, *AICHE journal* vol. 56, no. 11, pp. 2905-2912, 2010.
[42] Yu J. *et al.*, (2011) Biomass pyrolysis in a micro-fluidized bed reactor: characterization and kinetics, *Chemical engineering journal* vol. 168, no. 2, pp. 839-847, 2011.